Photodiagnosis and Photodynamic Therapy 26 (2019) 389–394

Contents lists available at ScienceDirect

Photodiagnosis and Photodynamic Therapy

journal homepage: www.elsevier.com/locate/pdpdt

The effect of C-X-C motif chemokine ligand 13 in cutaneous squamous cell carcinoma treated with aminolevulinic acid-photodynamic therapy

Lude Zhu[a], Guolong Zhang[b], Peiru Wang[b], Linglin Zhang[b], Jie Ji[b], Xiaojing Liu[b], Zhongxia Zhou[b], Jingjun Zhao[a,**], Xiuli Wang[b,*]

[a] Department of Dermatology, Tongji Hospital, Tongji University School of Medicine, Shanghai, China
[b] Institute of Photomedicine, Shanghai Skin Disease Hospital, Tongji University School of Medicine, Shanghai, China

ARTICLE INFO

Keywords:
5-Aminolevulinic acid-photodynamic therapy
C-X-C motif chemokine ligand 13
Cutaneous squamous cell carcinoma
Antitumor immunity

ABSTRACT

Background: Active recruitment of inflammatory cells into tumors may be vital for antitumor immunity in cutaneous squamous cell carcinoma (cSCC) after photodynamic therapy. Chemokines play important roles in inflammatory cell recruitment. Moreover, C-X-C motif chemokine ligand 13 (CXCL13) is thought to be a pivotal chemokine involved in inflammatory response and antitumor effect. Here, we examined the roles of CXCL13 in the response of cSCC to ALA-PDT.

Methods: Microarray analysis was used to select the chemokines involved in cSCC treated with ALA-PDT. The expression and transcriptional activity of CXCL13 were assessed by immunohistochemistry and quantitative real-time polymerase chain reaction. Western blotting was used to detect C-X-C motif chemokine receptor 5 (CXCR5) expression. The role of CXCL13 in ALA-PDT efficacy was assessed in vivo.

Results: Microarray analysis of total 63 chemokines and their receptors showed that the expression of 21 chemokines and 13 receptors were up-regulated in cSCC after ALA-PDT; in particular, CXCL13 was significantly upregulated. Immunohistochemistry showed that cancer-associated fibroblasts (CAFs) may be the main source of CXCL13 upregulation in the cSCC microenvironment after ALA-PDT. The efficacy of ALA-PDT in the treatment of cSCC was significantly reduced after CXCL13 inhibition.

Conclusion: CXCL13 plays important roles in the antitumor effect of ALA-PDT for cSCC and may originate mainly from CAFs in the cSCC microenvironment.

1. Introduction

Cutaneous squamous cell carcinoma (cSCC) is a common malignant tumor of the skin and is newly diagnosed in more than 1,000,000 patients annually in the USA, with increased incidence in elderly individuals [1]. Photodynamic therapy (PDT) is recommended for the treatment of cSCC in situ according to European guidelines [2]. Although PDT has been shown to have sufficient efficacy for treating superficial and micro-invasive cSCC [3–5], the recommendation for PDT in the treatment of invasive cSCC is debatable. Thus, further studies are needed to determine the mechanisms through which aminolevulinic acid (ALA)-PDT suppresses tumor growth in cSCC to identify targets for the development of ALA- PDT sensitizers.

The recruitment of an abundance of inflammatory cells in the tumor after PDT induces vitally active antitumor immunity to kill SCC cells [6–9]. Our previous animal study showed that the numbers of $CD4^+$ and $CD8^+$ lymphocytes are significantly increased in cSCC specimens after ALA-PDT [7]. Furthermore, PDT combined with imiquimod can enhance the efficacy for the treatment of invasive cSCC by inducing $CD8^+$ T cells [10]. Hence, exploration of the mechanisms of migration of these inflammatory cells is necessary. Chemokines are a superfamily of pro-inflammatory cytokines that selectively attract and activate different cell types. These molecules interact with seven-transmembrane-domain glycoprotein receptors coupled to the G protein signaling pathway [11]. Human cancers can utilize a complex chemokine network to influence tumor cell growth, death, migration, and metastasis [12–15]. Among these chemokines, C-X-C motif chemokine ligand 13 has been shown to be central component of immune-relevant metagenes, with a significant positive impact on antitumor responses [16]. CXCL13 is a member of the C-X-C motif chemokine subfamily that interacts with C-X-C motif chemokine receptor 5 (CXCR5) and is mainly expressed in cancer-associated fibroblasts (CAFs) in the tumor

* Corresponding author at: Institute of Photomedicine, Shanghai Skin Disease Hospital, 1278 Baode Road, Shanghai, 200443, China.
** Corresponding author.
E-mail addresses: zhaojingjun2015@aliyun.com (J. Zhao), wangxiuli_1400023@tongji.edu.cn (X. Wang).

https://doi.org/10.1016/j.pdpdt.2019.04.018
Received 23 January 2019; Received in revised form 20 March 2019; Accepted 19 April 2019
Available online 22 April 2019
1572-1000/

microenvironment [17]. However, the role of CXCL13 in the response of cSCC to aminolevulinic acid (ALA)- PDT has not been reported.

In this study, we performed microarray analysis to screen functional chemokines in cSCC treated with ALA-PDT. Then, we confirmed the upregulation of CXCL13 and examined its effect in the microenvironment of cSCC after ALA-PDT.

2. Material and methods

2.1. Ethical statement

The Institutional Research Medical Ethics Committee of Shanghai Skin Disease Hospital has approved this study (approval no. 2016-06). Written informed consent was obtained from all patients. All experimental protocols were performed according to the guidelines of the Declaration of Helsinki.

2.2. Mouse models

Female SKH-1 hairless mice (6–8 weeks old; Shanghai Public Health Clinic, China; Shanghai Certificate number 2010–0024) without skin injuries were used. There were two mouse models established in this study: primary cSCC mouse model and implanted cSCC mouse model.

First, nine mice were exposed to solar-simulated ultraviolet irradiation (Solar UV Simulator, Sigma Shanghai, China) on the back to induce primary cSCC as described previously [18]. This model was strictly simulating the natural formation process of human cSCC, so it approximately took 6 months for modeling. Moreover, the lesions of this mouse model were carpet-like and vary in size. When the tumor was up to 5 mm in diameter, it could be used for the study.

Second, XL50 cells (SCC cells; CCTCC no: C201827; Wuhan, China; 5×10^6) and NIH/3T3 cells (1×10^6) were injected subcutaneously into the backs of mice to establish an implanted cSCC mouse model. Unlike the primary cSCC mouse model, it only took 1 week and the tumor was single. Then, the tumor bearing mice could be used for the study when the tumor volume reached 10 mm in diameter.

2.3. PDT treatment and microarray analysis

Once the tumor volume of primary cSCC reached 10 mm in diameter, ALA- PDT was performed with 8% ALA cream applied at about 1-mm thickness. After 3 h of incubation, the lesions were irradiated with LED red light (630 nm, 30 J/cm^2) for 8 min. Nine paraffin-embedded specimens (control, n = 3; 3 h after ALA- PDT, n = 3; 6 h after ALA- PDT) were obtained from all nine mice. Total RNA was extracted from samples using TRIzol (Takara Bio, Inc., Otsu, Japan), according to the manufacturer's instructions. Microarray analysis was then conducted with the Affymetrix GeneChip Mouse Transcriptome Assay 1.0 (Affymetrix, Santa Clara, CA, USA) to detect the total gene expression of 63 chemokines. The data extracted using Feature Extraction software 9.5 were analyzed at the Gene-Cloud of Biotechnology Information (Genminix Informatics Ltd., Co.).

2.4. Patients and human specimens

Six patients with cSCC diagnosed by pathology were investigated in this study. Table 1 summarizes the characteristics of the patients. All patients rejected any other treatment, including surgery, and instead chose ALA- PDT because of their age and the location and size of the tumor. Twelve paraffin-embedded specimens (baseline, n = 6; 3 h after the first session of ALA-PDT, n = 6) were obtained from all six patients.

2.5. Treatment of human patients

All patients were examined for metastatic lesions before ALA- PDT. X-ray and computed tomography scanning showed no bone destruction or metastasis, except for patient number 3. After the discussion with the patient and his family about the potential application of multidisciplinary treatment (MDT), they still chose ALA-PDT as a palliative care approach to alleviate symptoms and maximize quality of life based on the location and the size of the lesion. ALA-PDT was then conducted as follows. First, scales and crusts were gently removed using paraffin oil and saline, and plum-blossom needling was used to tap the skin until spot bleeding occurred to facilitate ALA penetration [19]. Second, 20% 5-ALA cream (Shanghai Fudan- Zhangjiang Bio-pharmaceutical Co., Ltd, Shanghai, China) was applied for lesions with 2-cm margins for 4 h. Finally, the lesions were irradiated with red light (633 ± 6 nm; Omnilux Revive, Photo Therapeutics Ltd., Manchester, UK) at 100 mW/cm^2 (633 nm, 126 J/cm^2). Typically, 2% lidocaine was injected intradermally, and cold air was applied before and after irradiation, respectively, to relieve pain. Lesions were clinically examined, and photographs were taken to assess the treatment response. Additionally, dermoscopy was performed during each visit.

2.6. Extraction of total RNA and qRT-PCR

Total RNA was extracted from 12 human cSCC tissue samples and cell lines after ALA-PDTPDT using TRIzol (Takara Bio, Inc., Otsu, Japan), according to the manufacturer's instructions. The purity of total RNA was assessed using a spectrophotometer (Beckman, CA, USA). Reverse transcription of RNA into cDNA was performed using a Revert Aid First-Strand cDNA Synthesis Kit (Fermentas, CA, USA). qRT-PCR was conducted using a real-time detection system mix with SYBR Green (Syntol, Moscow, Russia) on a 7500 Fast Real-Time PCR System (Applied Biosystems, Foster City, CA, USA). Individual gene expression was normalized to the expression of glyceraldehyde 3-phosphate dehydrogenase (*GAPDH*). The designed primer sequences used to amplify human *CXCL13*, and *GAPDH* are listed in Table 2.

2.7. Western blot analysis

Production of CXCR5 was determined by western blotting using specimens from six patients (total of 12 samples). Total protein was extracted from human specimens using Tissue Total Protein Lysis Buffer (Sangon Biotech Co., Ltd., Shanghai, China), according to the manufacturer's protocol. A BCA Protein Assay Reagent kit (Thermo Fisher Scientific Inc., MA, USA) was used to quantify protein concentrations. Samples containing 40 μg of denatured total protein were fractionated

Table 1
Characteristics of cSCC patients included in this study.

No.	Age	Gender	Location	Tumor length (cm)	Differentiation	TNM stage	Recurrence	The risk of recurrence and metastasis
1	64	male	sole	2.8	high	T2N0M0	No	high
2	90	female	cheek	1.9	high	T1N0M0	No	high
3	78	male	perineum	10.0	high	T2N2cM1	Yes	high
4	92	male	finger	3.5	high	T2N0M0	No	high
5	87	female	heel	3.2	high	T2N0M0	No	high
6	57	male	lip	2.2	high	T2N0M0	No	high

Table 2
PCR primer sequences.

cDNA	Primer	Sequences
CXCL13	Forward	5′-GCTTGAGGTGTAGATGTGTCC-3′
	Reverse	5′-CCCACGGGGCAAGATTTGAA-3′
GAPDH	Forward	5′- CTGCACCACCAACTGC TT-3′
	Reverse	5′- TTCTGGGTGGCAG TGATG-3′

by sodium dodecyl sulfate polyacrylamide gel electrophoresis on 12% gels and transferred to polyvinylidene difluoride membranes. Membranes were then incubated overnight at 4 °C with anti-CXCR5 antibodies (1:1000 dilution; cat. no. ab46218; Abcam, Cambridge, MA, USA) and anti-GAPDH antibodies (1:2500 dilution; cat. no. ab9485; Abcam). After incubation with AP-conjugated secondary antibodies, the bands were visualized by enhanced chemiluminescence. Quantification of the results was carried out using GelPro Analysis Software (Media Cybernetics).

2.8. Immunohistochemistry

Immunohistochemistry for CXCL13 and vimentin was performed on formalin-fixed, paraffin-embedded human cSCC tissue sections (2 μm thickness). The slides were deparaffnized and then subjected to heat-induced antigen retrieval following rehydration through a graded ethanol series. After blocking endogenous peroxidases and endogenous biotin with 0.3% H_2O_2, the sections were incubated overnight with primary antibodies targeting CXCL13 (1:500 dilution; cat. no. ab227801; Abcam) and vimentin (1:1000 dilution; cat. no. ab45939; Abcam). The following day, after washing in phosphate-buffered saline (PBS), the slides were incubated with horseradish peroxidase-conjugated anti-rabbit secondary antibodies (1:250 dilution; Protein Tech, Chicago, IL, USA) for 30 min. Finally, the slides were developed with diaminobenzidine for 5 min and counterstained with hematoxylin.

2.9. Efficacy assessment in vivo

Once the tumor volume of tumor-implanted mice reached 10 mm in diameter, the mice were divided into four groups (five mice/group), as follows: (1) CXCL13 inhibition group, 50 μL anti- CXCL13 monoclonal antibodies (R&D, Minneapolis, MN, USA; 50 μg/mL) was injected into the tumor; (2) IgG control group, 50 μL IgG (R&D; 50 μg/mL) was injected into the tumor; (3) CXCL13 overexpression group, 50 μL recombinant mouse CXCL13 protein (R&D; 2 μg/mL) in PBS was injected into the tumor; and (4) PBS control group, 50 μL PBS was injected into the tumor. The intratumor injections in the four groups were all conducted 1 day before ALA-PDT, during PDT, and 6 and 24 h after ALA-PDT. ALA- PDT was performed on all tumor-implanted mice using the same protocol as described above. Baseline tumor volume was measured, and digital photographs were taken to assess the treatment efficacy. After one treatment, tumor volumes were measured every 2 days, and photographs were taken twice a week for 2 weeks. Tumor volumes were calculated with the formula $V = (\text{length} \times \text{width}^2) / 2$. Mice were euthanized when the volume of the largest tumor exceeded 1500 mm^3.

2.10. Statistical analysis

Statistical analysis was performed using SPSS13.0 (SPSS, Chicago, IL, USA). All quantitative data were recorded as means ± standard deviations. Comparisons between two groups were conducted using t tests, and *P* values of less than 0.05 denoted statistical significance.

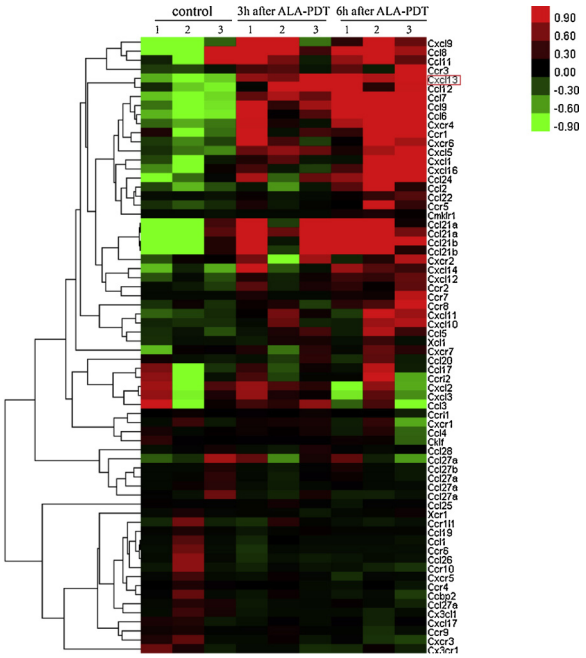

Fig. 1. Microarray analysis. The samples of primary cSCC (control, n = 3; 3 h after ALA-PDT, n = 3; 6 h after ALA-PDT) were obtained from the primary cSCC mouse model. The heat map revealed the change of gene expression of total 63 chemokines in cSCC after ALA-PDT. A color scale was used to represent the gene expression level: red for highly expressed genes and green for lowly expressed genes.

3. Results

3.1. Microarray analysis and chemokine screening

Recruitment of an abundance of inflammatory cells is the key to host antitumor immunity in cSCC after treatment with ALA-PDT [6–8]. To explore which chemokines were critical in the tumor microenvironment after ALA-PDT, a microarray analysis of 63 chemokines and their receptors was conducted. As shown in Fig. 1, the expression levels of 21 chemokines and 13 receptors were increased in tumors after ALA-PDT. Among these chemokines, CXCL13 was significantly upregulated after ALA-PDT with a small standard deviation. Thus, it is meaningful to study the role of CXCL13 in cSCC after ALA-PDT.

3.2. Upregulation of CXCL13 and its receptor CXCR5 after ALA-PDT in cSCC

QRT-PCR was performed to verify CXCL13 expression after ALA-PDT in patients. As shown in Fig. 2a, the expression of CXCL13 was upregulated at 3 h after ALA-PDT compared with that at baseline. Moreover, immunohistochemistry and western blot analysis were performed to detect CXCL13 and CXCR5 protein expression. As shown in Fig. 2c, the number of $CXCL13^+$ cells increased at 3 h after treatment compared with that at baseline. Additionally, western blotting results in Fig. 2b showed that there were clear increases in CXCR5 at 3 h after treatment compared with that at baseline. Our data suggested that CXCL13 and its receptor CXCR5 were upregulated in the cSCC microenvironment after ALA-PDT.

3.3. Cancer-associated fibroblasts (CAFs) mainly expressed CXCL13 after ALA-PDT in cSCC

CXCL13 is mainly expressed by CAFs in the tumor microenvironment [17,20,21]. To determine the main source of CXCL13, immunohistochemistry of mesenchymal cells was performed using

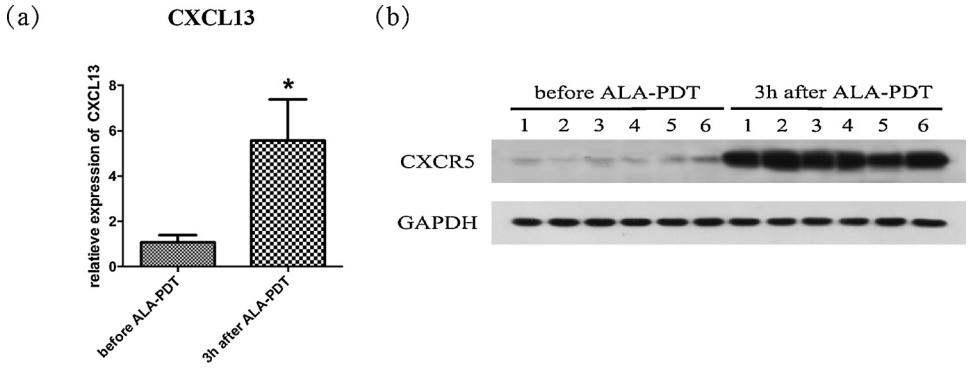

Fig. 2. ALA-PDT promotes the production of chemokine CXCL13. (a) Total RNA was extracted from six patients, and qRT-PCR was conducted to detect the expression of chemokine CXCL13. **(b)** Whole human cSCC tissues extracts were probed by Western blot for CXCR5. **(c)** Immunohistochemistry was used to detect the expression of CXCL13 before and 3 h after ALA-PDT in human cSCC tissues. GAPDH is shown as a loading control. *Significant increase ($p < 0.05$). Results are representative of three similar experiments. Original magnification: X 100.

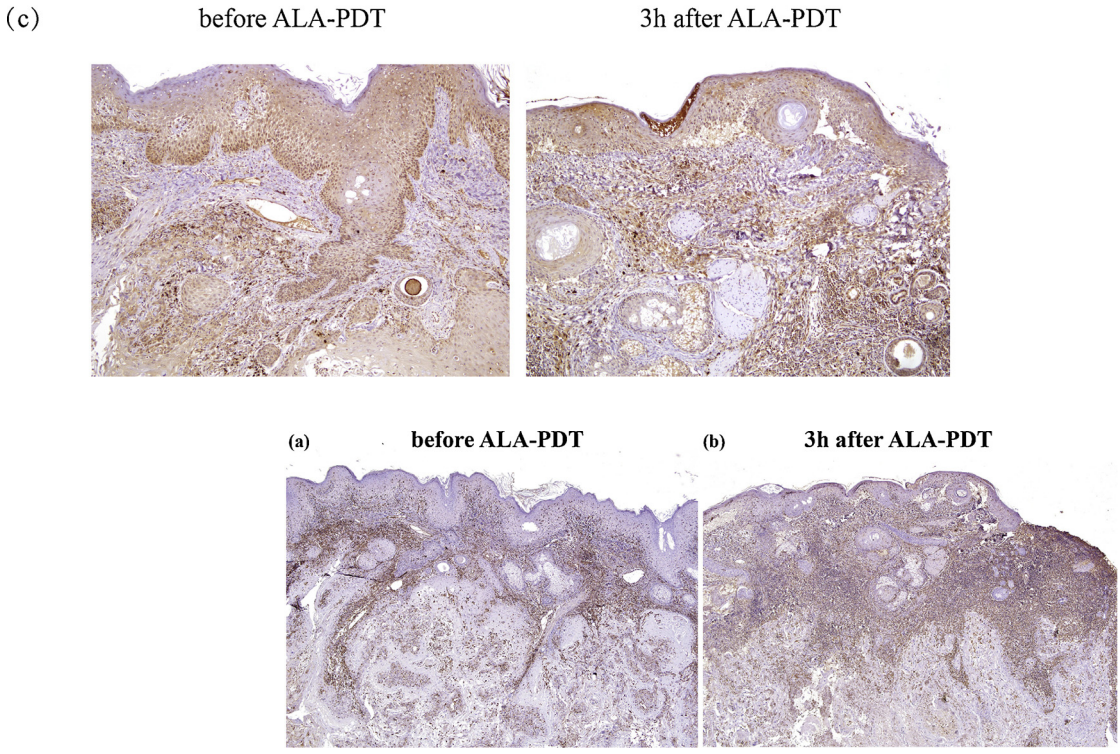

Fig. 3. CAFs expressed CXCL13 after ALA-PDT in cSCC. Immunohistochemistry was used to detect vimentin **(a)** before and **(b)** 3 h after ALA-PDT in human cSCC tissues. Original magnification: X 100.

vimentin as a marker. Notably, the number of mesenchymal cells was increased in cSCC after ALA-PDT (Fig. 3). These data suggested that CAFs may be the main source of CXCL13 upregulation in the cSCC microenvironment after ALA-PDT.

3.4. CXCL13 was critical for therapeutic efficacy

To examine whether CXCL13 enhanced the efficacy of ALA-PDT in mice harboring cSCC-derived tumors, tumor volumes were compared in the CXCL13 inhibition group, IgG control group, CXCL13 overexpression group, and PBS control group. As shown in Fig. 4, there were no significant differences in tumor volumes between the IgG and PBS control groups, and one mouse was completely cured in each group. In the CXCL13 overexpression group, tumor volumes were significantly decreased over time, and two mice showed complete elimination of tumors. However, in the CXCL13 inhibition group, the tumor volume was significantly greater than that in the CXCL13 overexpression group. Images of tumors on the final day of the experiment are shown in Fig. 4. Overall, these results suggested that CXCL13 played a critical role in modulating the therapeutic efficacy of ALA-PDT for cSCC.

4. Discussion

ALA-PDT has been applied for the treatment of actinic keratosis (AK), cSCC in situ, and basal cell carcinoma. However, the absorption of photosensitizers and depth of light source illumination are limited; thus, ALA-PDT may not be recommended for the treatment of cSCC. Conventional treatments, such as surgery, directly removes or destroys the tumor tissue. Such processes are invasive, associated with frequent relapse, and can cause difficulties with follow-up treatment after recurrence in elderly individuals [22]. ALA-PDT also may have the advantage of cosmetic effects and functional retention in cSCC [23]. Therefore, exploration of the mechanisms through which ALA-PDT exerts antitumor effects in cSCC is essential.

Increasing evidence has shown that chemokines and their receptors have significant antitumor effects [24]. Therefore, a microarray analysis of 63 chemokine genes was performed to screen functional chemokines and their receptors in cSCC treated with ALA-PDT. The results showed that 21 chemokines and 13 receptors were upregulated in tumors after ALA-PDT. Among these chemokines, CXC-chemokines (e.g., CXCL9 and CXCL13) and CC-chemokines (e.g., CCL8, CCL11, CCL12, CCL7, CCL9, CCL6) were apparently upregulated. These data suggested

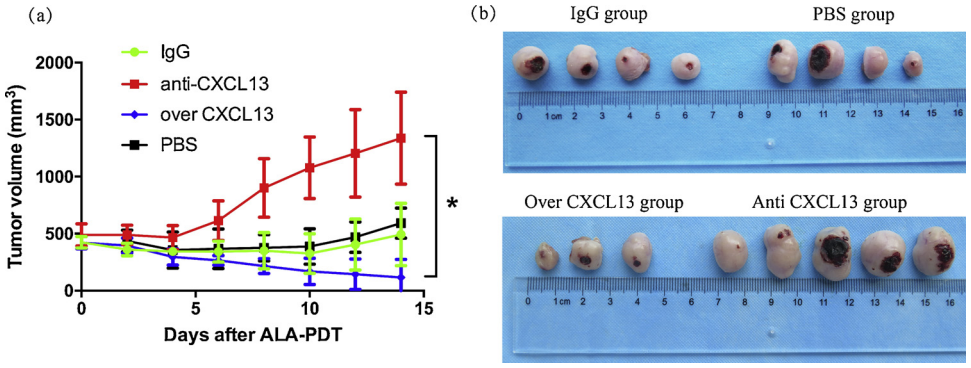

Fig. 4. CXCL13 is critical for the ALA-PDT therapeutic efficacy of cSCC. Twenty female SKH-1 hairless mice (6–8 weeks old) were used. XL50 (SCC cell) cells (5×10^6) and NIH/3T3 cells (1×10^6) were injected subcutaneously into the backs of the mice to establish an implanted cSCC mouse model. When the tumor volume reached 10 mm in diameter ($V = 500mm^3$), all tumor-bearing mice were divided into four groups (5 mice/group). The intra-tumor injections in the four groups were all conducted 1 day before ALA-PDT, during PDT, and 6 and 24 h after ALA-PDT. Baseline tumor volume was measured, and digital photographs were taken to assess the treatment efficacy. **(a)** After one treatment, tumor volumes were measured every 2 days, and photographs were taken twice a week for 2 weeks. Tumor volumes were calculated with the formula $V = (\text{length} \times \text{width}^2) / 2$. **(b)** Until the biggest tumor volume was close to 1500 mm^3, all mouse was executed. Results are expressed as means ± SEM.

that chemokines play important roles in cSCC treated with ALA–PDT. In particular, the expression of CXCL13 was significantly upregulated, with a small standard deviation. Immunohistochemistry and qRT-PCTwere conducted to confirm the expression and transcriptional activity of CXCL13 in human cSCC treated with ALA-PDT. This, CXCL13 may be a key factor in the tumor microenvironment after ALA-PDT.

CXCL13 is also known as a B cell-attracting-1(BCA-1) that can attract $CXCR5^+$ B cells, $CD4^+$ and $CD8^+$ T cells, dendritic cells (DCs), follicular T helper cells (Tfh), and macrophages by interacting with CXCR5 [11,25,26]. CXCL13 can be derived from different cells under various disease conditions. For example, in inflammatory diseases, CXCL13 is mainly produced by dendritic cells and macrophages [27]. In contrast, in tumors, CXCL13 is primarily produced by CAFs [20,21]. In this study, our data also suggested that CAFs may be the main source of CXCL13 upregulation in the cSCC microenvironment after ALA-PDT.

CXCL13 is generally thought to be a tumor-promoting protein. Moreover, this protein acts as a positive regulator of tumor invasion and the epithelial-to-mesenchymal transition by promoting the migration of $CXCR5^+$ tumor cells [17]. Previous studies have suggested that tissue injury and hypoxia promote the development of prostate cancer by inducing CXCL13 expression in CAFs [21]. However, our data showed that CXCL13 played a critical role in modulating the therapeutic efficacy of ALA-PDT for cSCC. Similar debates have been reported in breast cancer [28,29] and different types of SCC [30–32]. CXCL13 can promote lymph node metastasis in breast cancers [33], and its expression is also associated with a better disease-free survival rate after neoadjuvant chemotherapy in patients with triple-negative breast cancer (TNBC) [29]. In addition, in oral squamous cell carcinoma, CXCL13 has functional roles in bone invasion and may be a potential therapeutic target [30,31]. However, CXCL13 has the opposite function in esophageal squamous cell carcinoma via enhancement by interleukin-17 A [32]. Thus, CXCL13 could play two opposing roles (promotion and inhibition) in the tumor microenvironment. Chen et al. suggested that differences in race, age, and disease can lead to differences in the tumor microenvironment, causing some chemokines to have completely different functions than typically observed [34]. Notably, in this study, ALA-PDT may disrupt the tumor microenvironment in cSCC via the functions of CXCL13. Indeed, we found that ALA-PDT could induce CXCL13 causing antitumor immunity in cSCC. Further studies using more mouse models are needed to confirm these findings.

In conclusion, we found that CXCL13 and its receptor CXCR5 were significantly upregulated following ALA-PDT. Additionally, CAFs may be the main source of upregulated CXCL13 in the cSCC microenvironment after ALA-PDT. Most importantly, the efficacy of ALA-PDT for cSCC was significantly reduced after inhibition of CXCL13, suggesting that CXCL13 played a critical role in mediating the therapeutic efficacy of ALA-PDT for cSCC. These findings provide important insights into the application of ALA-PDT and may facilitate the identification of novel PDT-sensitizing agents.

Ethics approval

This study was conducted with the approval of The Institutional Research Medical Ethics Committee of Shanghai Skin Disease Hospital (2016-06).

Funding

This study was supported by National Natural Science Foundation of China (81872212 and 81602396), Tutor training program (17HBDS04), Shanghai Pujiang Program (17PJ1408500) and Talent youth program of Shanghai Health and Family planning system (2017YQ066).

Conflicts of interest

The authors have no conflicts of interest to disclose.

References

[1] G.P. Guy Jr., S.R. Machlin, D.U. Ekwueme, et al., Prevalence and costs of skin cancer treatment in the U.S., 2002-2006 and 2007-2011, Am. J. Prev. Med. 48 (2) (2015) 183–187.
[2] A.M. Skaria, European guidelines for topical PDT part 1 JEADV 2013; 27: 536-544, J. Eur. Acad. Dermatol. Venereol. 28 (5) (2014) 673.
[3] S.H. Choi, K.H. Kim, K.H. Song, Effect of methyl aminolevulinate photodynamic therapy with and without ablative fractional laser treatment in patients with microinvasive squamous cell carcinoma: a randomized clinical trial, JAMA Dermatol. 153 (3) (2017) 289–295.
[4] M.C. Fargnoli, D. Kostaki, A. Piccioni, et al., Photodynamic therapy for the treatment of microinvasive squamous cell carcinoma of the lower lip: a case report, G. Ital. Dermatol. Venereol. 150 (3) (2015) 331–335.
[5] A. Sidoroff, Photodynamic therapy of cutaneous epithelial malignancies. An evidence-based review, Hautarzt 58 (7) (2007) 577–584.
[6] M.T. Wan, J.Y. Lin, Current evidence and applications of photodynamic therapy in dermatology, Clin. Cosmet. Investig. Dermatol. 7 (2014) 145–163.
[7] H. Wang, J. Li, T. Lv, et al., Therapeutic and immune effects of 5-aminolevulinic acid photodynamic therapy on UVB-induced squamous cell carcinomas in hairless mice, Exp. Dermatol. 22 (5) (2013) 362–363.
[8] A.D. Garg, P. Agostinis, ER stress, autophagy and immunogenic cell death in photodynamic therapy-induced anti-cancer immune responses, Photochem. Photobiol. Sci. 13 (3) (2014) 474–487.
[9] A.D. Garg, D. Nowis, J. Golab, et al., Photodynamic therapy: illuminating the road from cell death towards anti-tumour immunity, Apoptosis 15 (9) (2010) 1050–1071.
[10] A.K. Bhatta, P. Wang, U. Keyal, et al., Therapeutic effect of Imiquimod enhanced ALA-PDT on cutaneous squamous cell carcinoma, Photodiagnosis Photodyn. Ther. 23 (2018) 273–280.
[11] A. Zlotnik, O. Yoshie, Chemokines: a new classification system and their role in immunity, Immunity 12 (2) (2000) 121–127.
[12] E.C. Keeley, B. Mehrad, R.M. Strieter, CXC chemokines in cancer angiogenesis and metastases, Adv. Cancer Res. 106 (2010) 91–111.
[13] A.P. Vicari, C. Caux, Chemokines in cancer, Cytokine Growth Factor Rev. 13 (2) (2002) 143–154.
[14] T. Murakami, A.R. Cardones, S.T. Hwang, Chemokine receptors and melanoma

metastasi, J. Dermatol. Sci. 36 (2) (2004) 71–78.
[15] E. Marcuzzi, R. Angioni, B. Molon, et al., Chemokines and chemokine receptors: orchestrating tumor metastasization, Int. J. Mol. Sci. 20 (1) (2018).
[16] G. Stoll, D. Enot, B. Mlecnik, et al., Immune-related gene signatures predict the outcome of neoadjuvant chemotherapy, Oncoimmunology 3 (1) (2014) e27884.
[17] S. Biswas, S. Sengupta, S. Roy Chowdhury, et al., CXCL13-CXCR5 co-expression regulates epithelial to mesenchymal transition of breast cancer cells during lymph node metastasis, Breast Cancer Res. Treat. 143 (2) (2014) 265–276.
[18] X. Wang, L. Shi, Q. Tu, et al., Treating cutaneous squamous cell carcinoma using 5-aminolevulinic acid polylactic-co-glycolic acid nanoparticle-mediated photodynamic therapy in a mouse model, Int. J. Nanomedicine 10 (2015) 347–355.
[19] J. Chen, Y. Zhang, P. Wang, et al., Plum-blossom needling promoted PpIX fluorescence intensity from 5-aminolevulinic acid in porcine skin model and patients with actnic keratosis, Photodiagnosis Photodyn. Ther. 15 (2016) 182–190.
[20] C.G. Mueller, S. Nayar, J. Campos, et al., Molecular and cellular requirements for the assembly of tertiary lymphoid structures, Adv. Exp. Med. Biol. 1060 (2018) 55–72.
[21] M. Ammirante, S. Shalapour, Y. Kang, et al., Tissue injury and hypoxia promote malignant progression of prostate cancer by inducing CXCL13 expression in tumor myofibroblasts, Proc. Natl. Acad. Sci. U. S. A. 111 (41) (2014) 14776–14781.
[22] J.J. Bonerandi, C. Beauvillain, L. Caquant, et al., Guidelines for the diagnosis and treatment of cutaneous squamous cell carcinoma and precursor lesions, J. Eur. Acad. Dermatol. Venereol. 25 (Suppl 5) (2011) 1–51.
[23] M. Oran, C. Unsal, Y. Albayrak, et al., Possible association between vitamin D deficiency and restless legs syndrome, Neuropsychiatr. Dis. Treat. 10 (2014) 953–958.
[24] S. Cabrero-de Las Heras, E. Martinez-Balibrea, CXC family of chemokines as prognostic or predictive biomarkers and possible drug targets in colorectal cancer, World J. Gastroenterol. 24 (42) (2018) 4738–4749.
[25] B. Leon, A. Ballesteros-Tato, J.L. Browning, et al., Regulation of T(H)2 development by CXCR5+ dendritic cells and lymphotoxin-expressing B cells, Nat. Immunol. 13 (7) (2012) 681–690.
[26] B. Halvorsen, L.M. Smedbakken, A.E. Michelsen, et al., Activated platelets promote increased monocyte expression of CXCR5 through prostaglandin E2-related mechanisms and enhance the anti-inflammatory effects of CXCL13, Atherosclerosis 234 (2) (2014) 352–359.
[27] K. Neyt, F. Perros, C.H. GeurtsvanKessel, et al., Tertiary lymphoid organs in infection and autoimmunity, Trends Immunol. 33 (6) (2012) 297–305.
[28] O. Tudoran, O. Virtic, L. Balacescu, et al., Baseline blood immunological profiling differentiates between Her2-breast cancer molecular subtypes: implications for immunomediated mechanisms of treatment response, Onco. Ther. 8 (2015) 3415–3423.
[29] I.H. Song, S.H. Heo, W.S. Bang, et al., Predictive value of tertiary lymphoid structures assessed by high endothelial venule counts in the neoadjuvant setting of triple-negative breast Cancer, Cancer Res. Treat. 49 (2) (2017) 399–407.
[30] Y. Sambandam, K. Sundaram, A. Liu, et al., CXCL13 activation of c-Myc induces RANK ligand expression in stromal/preosteoblast cells in the oral squamous cell carcinoma tumor-bone microenvironment, Oncogene 32 (1) (2013) 97–105.
[31] S.N. Pandruvada, S. Yuvaraj, X. Liu, et al., Role of CXC chemokine ligand 13 in oral squamous cell carcinoma associated osteolysis in athymic mice, Int. J. Cancer 126 (10) (2010) 2319–2329.
[32] L. Lu, C. Weng, H. Mao, et al., IL-17A promotes migration and tumor killing capability of B cells in esophageal squamous cell carcinoma, Oncotarget 7 (16) (2016) 21853–21864.
[33] S. Irshad, F. Flores-Borja, K. Lawler, et al., RORgammat(+) innate lymphoid cells promote lymph node metastasis of breast cancers, Cancer Res. 77 (5) (2017) 1083–1096.
[34] L. Chen, Z. Huang, G. Yao, et al., Erratum to: the expression of CXCL13 and its relation to unfavorable clinical characteristics in young breast cancer, J. Transl. Med. 14 (1) (2016) 318.